Improving Shewhart-type Generalized Variance Control Charts for Multivariate Process Variability Monitoring using Cornish-Fisher Quantile Correction, Meijer-G Function and Other Tools

Emanuel P. Barbosa[1], Mario A. Gneri, Ariane Meneguetti

Depto Estatística, IMECC-UNICAMP, Campinas, SP, Brazil

Abstract

This paper presents an improved version of the Shewhart-type generalized variance $|S|$ control chart for multivariate Gaussian process dispersion monitoring, based on the Cornish-Fisher quantile formula for non-normality correction of the traditional normal based 3-sigma chart limits.

Also, the exact sample distribution of $|S|$ and its quantiles (chart exact limits) are obtained through the Meijer-G function (inverse Mellin-Barnes integral transform), and an auxiliary control chart based on the trace of the standardized S matrix is introduced in order to avoid non detection of certain changes in the process variance-covariance Σ matrix.

The performance of the proposed CF-corrected control chart is compared, considering false alarm risk (using analytical and simulation tools), with the traditional normal based chart and with the exact distributed based chart (for dimensions $d = 2$ and $d = 3$). This study shows that the proposed control limit corrections do remove the drawback of excess of false alarm associated with the traditional normal based $|S|$ control chart.

The proposed new chart (with its corresponding auxiliary chart) is illustrated with two numerical examples.

Keywords Cornish-Fisher, False Alarm, Generalized Variance, Meijer-G function, Multivariate Process, Variability Monitoring.

1 Introduction

The modern statistical process control took place when Walter A. Shewhart in 1926 developed the concept of a control chart based on the monitoring of the process mean level

[1]Address correspondence to Emanuel P. Barbosa, IMECC, UNICAMP, Barão Geraldo, 13083-859, Campinas, SP, Brazil; E-mail: emanuel@ime.unicamp.br

through sample mean ($\bar{X}$ chart) and process dispersion through sample Range (R chart) or sample Standard Deviation chart. In the multivariate setting, the basic monitoring tools for process level and process variability, are respectively the Hotelling T^2 statistic (Hotelling, 1931, 1947) and the statistics based on the sample variance-covariance S matrix. For an inroduction to multivariate statistical process control, see for instance, Fuchs and Kenett (1998), Mason and Young (2001) or Kruger and Xie (2012). For a general discussion of multivariate control charts for variance-covariance matrix monitoring, see also Yeh et al. (2006). The two more important and used statistics based on the sample variance-covariance S matrix, for process variability monitoring and testing, are the Likelihood-Ratio (LR) and the Generalized Variance (GV) given by $|S|$, the determinant of S (Wilks, 1932; Anderson, 1958; Korin, 1968; Alt, 1984; Aparisi et al, 1999; Dogu and Kocakoç, 2011).

The study of control charts for multivariate Gaussian process variability monitoring based on the sample generalized variance $|S|$ statistic has received attention in the literature (for instance, Alt, 1984; Aparisi et al, 1999; Djauhari, 2005; Djauhari et al, 2008 and others), and it is the object of the present paper.

Although this statistic is considered simpler than the LR for applications in control charts, there are two important drawbacks in its use for process monitoring. The first one concerns its theoretical properties, since the process variance-covariance Σ matrix can change without necessarily changing its determinant (see Johnson and Wichern, 1982 or Aparisi et al, 1999) and so, S can change significantly (reflecting a change in Σ) without any change in $|S|$. The other one concerns its practical implementation, since asymptotic results for the sampling distribution of $|S|$ based on normal approximation to the exact distribution do not work well for small or moderate sample sizes, because the convergence to the normal is extremely slow (it would need extremely large sample sizes, such as, say, one thousand or more). The theoretical limitation can be alleviated with joint use of $|S|$ and some other auxiliary charts such as univariate variance charts and/or charts based on the S matrix through a function of its trace (see Alt, 1984; Aparisi et al, 1999; Djauhari et al, 2008).

How to overcome these two difficulties (practical and theoretical) is shown here in detail. The question is that the exact distribution of the sample $|S|$ does not have a simple form for dimension $d > 2$ (Mathai, 1972; Pham-Gia and Turkkan, 2010) and it is common to approximate it by a normal distribution, as in Alt (1984), Djauhari (2005, 2008), Montgomery (2008) and others, considering a sort of 3-sigma limits (Shewhart type) control charts. However, this sort of normal approximation, although very used in practice, is not proper, since it has a very serious drawback: it produces a severe increase in the false alarm risk (what is shown in this paper at section 4) as a consequence of misplaced control limits. For a general discussion of misplaced limits in control charts and the interpretation of control charts as hypothesis tests tools, see Alwan and Roberts (1995) and Woodall (2000).

The solution we present here to overcome this drawback is to work with a very good approximation to the exact distribution of $|S|$, correcting its non-normality through the Cornish-Fisher (CF) quantile expansion formula (see Cornish and Fisher, 1960; Lee and Lee, 1992, or the site www.riskglossary.com). Some references about using the CF quantile correction in the context of univariate control charts include, among others, Winterbottom (1993), Chan and Cui (2003), Cavalcanti and Cordeiro (2006), Joekes and Barbosa (2013). A reference for CF in the context of Multivariate Analysis (MA) is Fujikoshi et al (2010), but it just mention CF without applying it to the GV statistic (other MA textbooks even mention CF).

In fact, we haven't found any reference about the use of CF quantile correction in the context of multivariate control charts or the GV satistic. However, the actual context, where we know the GV moments or all orders is adequate for using this tool for quantile (chart limits) correction, in order to keep the false alarm risk under control (pre-fixed level). The information provided by the 3^{rd} (and 4^{th} order at most) moments or cumulants of the $|S|$ sample distribution will be sufficient for a satisfactory approximation. The exact distribution, although difficult to implement, can be expressed through the Meijer-G function (Springer, 1979) since it involves the product of independent chi-square distributions (Anderson, 1984). Also, to overcome the theoretical limitation of the generalized variance statistic (not detecting some changes on the variance covariance Σ matrix) we consider its joint use with an auxiliary statistic given by the trace of standardized S matrix (V matrix). These two statistics, based on determinant and trace of sample covariance matrix, are the two data components of the likelihood ratio statistic (Anderson, 1984; Seber, 1984 and Korin, 1968) for monitoring and testing if Σ is equal to a given Σ_0 (process dispersion matrix under control conditions). The procedures proposed here based on CF correction are effective and simple, for quality problems of low or moderate dimension and sample sizes not extremely small ($n > 10$, say), useful mainly in applications related to manufacturing (discrete parts processes); otherwise we can use the $|S|$ exact distribution through the Meijer-G function.

The organization of the paper is the following. The standard normal based $|S|$ control chart and corresponding moments formulae are reviewed in section 2, as well as the introduction to the Meijer-G function. The new $|S|$ control chart based on the Cornish-Fisher correction is presented at section 3 with special emphasis to the cases of dimensions $d = 2$ and $d = 3$, followed by the introduction of the $tr(V)$ chart. A false alarm comparative study to show the advantages of the new chart in relation to the traditional one, is presented in section 4. The proposed new chart is illustrated with a couple of numerical examples in section 5. Final comments and conclusions are presented in section 6, further research at section 7, followed by the references.

2 The Normal-based $|S|$ Control Chart

2.1 The Sample $|S|$ and Its Basic Properties

(i) **notation and definition:** Let $(X_1, X_2, ..., X_n)$ be a random sample from a d-variate normal with parameters μ and Σ, for $n = 2, 3, ...$ and $d = 2, 3, ...$ Then, the statistics *sample mean vector* $\bar{X}$ and *sample variance-covariance matrix* S, are:

$$\bar{X} = \frac{1}{n}\sum_{i=1}^{n} X_i \quad ; \qquad S = \frac{1}{n-1}\sum_{i=1}^{n}(X_i - \bar{X})(X_i - \bar{X})^T$$

The sample generalized variance, is $|S| = determinant(S)$.

(ii) **distribution:** From Anderson, T.W. (1958, 1984, 2003), it is known that, $|S|$ has the same distribution of $\frac{|\Sigma|}{(n-1)^d} Z_1 Z_2 ... Z_{\mathrm{d}}$ where $Z_k \sim \chi^2_{n-k}$ are independent, $k = 1, 2, ..., d$. As a consequence, when $d = 2$, we have (Anderson, 1958, 1984; Alt, 1984; Aparisi et al, 1999), $|S| \sim \frac{|\Sigma|}{4(n-1)^2}(\chi^2_{2n-4})^2$. In general for $d \geq 2$, the $|S|$ sampling distribution can be obtained numerically by simulation of S, using a Wishart generator algorithm (Smith and Hocking, 1972) through the software Matlab or R for instance. See Figure 4 in Subsection 4.2.

Also, since each of the d chi-square variables in the distribution of $|S|$ can be expressed in terms of the Meijer G-function (Bateman and Edéryi, 1953; Springer, 1979), with density given by

$$h_{Z_i}(z) = \frac{1}{2\,\Gamma(\frac{n-i-1}{2})}\, G^{\,1\ 0}_{0\ 1}\left(\frac{z}{2} \mid \frac{(n-i-2)}{2}\right) \quad i = 1, 2, ..., d \quad ,$$

then, since the product of independent G-function distributions is also a G-function, we have:

$$h(y) = \frac{1}{2^d}\left(\prod_{i=1}^{d} \frac{1}{\Gamma(\frac{n-i-1}{2})}\right) G^{\,d\ 0}_{0\ d}\left(\frac{y}{2^d} \mid \frac{(n-3)}{2}, \frac{(n-4)}{2}, ..., \frac{(n-d-2)}{2}\right) \quad , \ y > 0$$

where $Y = Z_1 Z_2 ... Z_d$ and G with the 2×2 matrix superscript is the special function called Meijer G, which is the inverse Mellin-Barnes integral transform of a quotient of products of gamma functions (moments function in the statistical context). The moments function of $|S|$ is presented in iii) and the Mellin transform definition is presented in v) of this subsection. See Springer, M. (1979) for a more general definition and other properties of the G function.

Although this function is not yet implemented in statistical software packages, it can be implemented using the recent version of the Symbolic Math Toolbox of Matlab. The exact quantile of interest for the one-sided $|S|$ control chart is the value $\frac{|\Sigma| y_0}{(n-1)^d}$ such that

$$\int_0^{y_o} h(y)dy = 1 - \alpha.$$

Some exact upper quantiles for $\alpha = 0.0020$ and $\alpha = 0.0027$, for dimension $d = 3$, are given in Table 1.

Table 1: **Exact values of scaled quantiles** $x_0 = \frac{y_0}{(n-1)^d}$

$d = 3$, $\alpha_0 = 0.0020$ **and** 0.0027

n	$1-\alpha_0$		n	$1-\alpha_0$	
	0.9980	**0.9973**		**0.9980**	**0.9973**
4	6.111	5.370	10	4.908	4.588
5	6.453	5.828	11	4.673	4.383
6	6.200	5.656	12	4.468	4.202
7	5.833	5.375	13	4.287	4.042
8	5.487	5.084	14	4.127	3.900
9	5.180	4.822	15	3.985	3.772

(iii) **moments (ordinary and central) and asymptotic distribution:** From the general expression above for $|S|$, and using moment formulas for χ^2 r.v., it is obtained the r$^{\text{th}}$ (ordinary) moment formulae or moment function (Anderson, 1958, 1984):

$$\alpha_r = \mathbb{E}\left(|S|^r\right) = \left(\frac{2}{n-1}\right)^{dr} |\Sigma|^r \prod_{k=1}^{d} \frac{\Gamma(r + \frac{n-k}{2})}{\Gamma(\frac{n-k}{2})}$$

In particular, the first four ordinary moments are given by:

$$\alpha_1 = \mathbb{E}\left(|S|\right) = \frac{|\Sigma|}{(n-1)^d} \prod_{k=1}^{d} (n-k) \quad ; \quad \alpha_2 = \mathbb{E}\left(|S|^2\right) = \frac{|\Sigma|^2}{(n-1)^{2d}} \prod_{k=1}^{d} (n-k+2)(n-k)$$

$$\alpha_3 = \mathbb{E}\left(|S|^3\right) = \frac{|\Sigma|^3}{(n-1)^{3d}} \prod_{k=1}^{d} (n-k+4)(n-k+2)(n-k)$$

$$\alpha_4 = \mathbb{E}\left(|S|^4\right) = \frac{|\Sigma|^4}{(n-1)^{4d}} \prod_{k=1}^{d} (n-k+6)(n-k+4)(n-k+2)(n-k)$$

The central moments are given by:

$$\mu_k = \mathbb{E}\left(|S| - \mu\right)^k = \sum_{r=0}^{k} \alpha_r \binom{k}{r} (-\mu)^{k-r} \text{ ; for } k = 1, 2, 3, 4, \text{ we have,}$$

$$\mu = \alpha_1 = \mathbb{E}\left(|S|\right) \quad , \quad \mu_2 = \alpha_2 - \alpha_1^2 = Var\left(|S|\right)$$

$$\mu_3 = \alpha_3 - 3\alpha_1\alpha_2 + 2\alpha_1^3 \quad , \quad \mu_4 = \alpha_4 - 4\alpha_3\alpha_1 + 6\alpha_2\alpha_1^2 - 3\alpha_1^4$$

The asymptotic distribution of $|S|$ is known to be Gaussian (Anderson, 1958, 1984) with moments $\mu = \alpha_1 = E(|S|)$ and $\sigma^2 = \mu_2 = Var(|S|)$. However, this sort of approximation to the exact $|S|$ sampling distribution is very bad (see Figures 1, 2, 3 and 5 at Section 4), and a quantile correction is presented in subsection 3.1 using the information given by the cumulants.

(iv) **cumulants:** From the Cumulants Generating Function (logarithm of the moments generating function), with the central moments previouslly standardized, we have:

$$K_1 = \mu^* = \frac{\alpha_1}{\sigma} \quad , \quad K_2 = \mu_2^* = \frac{\mu_2}{\sigma^2} \quad , \quad K_3 = \mu_3^* = \frac{\mu_3}{\sigma^3} \quad , \quad K_4 = \mu_4^* - 3\mu_2^{*2} = \frac{\mu_4}{\sigma^4} - 3\left(\frac{\mu_2}{\sigma^2}\right)^2$$

where $\sigma = \sqrt{\mu_2}$.

(v) **Mellin integral transforms and Meijer G-function**: the Mellin tranform of the density function $h(y)$, $0 < y < \infty$, of a random variable Y, is defined to be (Kabe, 1958)

$$g(s) = \int_0^\infty y^{s-1} h(y) dy \qquad \text{and its inverse transformation}$$

$$h(y) = \frac{1}{2\pi i} \int_{-i\infty}^{i\infty} y^{-s} g(s) ds \qquad \text{(Mellin-Barnes integral)}$$

where $i = \sqrt{-1}$ and $g(s)$ is the ordinary moment of order $s-1$ of Y (moment function). When this moment function has the form of a quotient of products of gamma functions (which is the case of $Y = |S|$, shown in (iii)), the inverse Mellin transform is called a Meijer G function. Its main property is that the product of G functions from independent random variables is also a G function itself. Fore more details, see Springer (1979).

2.2 Normal $|S|$ Control Chart: Limits and False Alarm Risk

(i) **limits:** From the moments formulae of section 2.1, the traditional 3-sigma control limits for the $|S|$ chart, in the case of $d = 2$, are given by,

$$\mathbb{E}(|S|) \pm 3\sqrt{Var(|S|)} = |\Sigma| \left(b_1 \pm 3\sqrt{b_2}\right) \text{ , where } b_1 = \frac{(n-2)}{(n-1)} \text{ and } b_2 = \frac{(n-2)(4n-2)}{(n-1)^3}$$

In the general d-dimensional case, we have the same expressions for the control limits (Lower and Upper Control Limits),

$$LCL = |\Sigma| \left(b_1 - 3\sqrt{b_2}\right) \quad ; \quad UCL = |\Sigma| \left(b_1 + 3\sqrt{b_2}\right)$$

but now, b_1 and b_2 are given by,

$$b_1 = \frac{1}{(n-1)^d} \prod_{i=1}^{d} (n-i) \quad ; \quad b_2 = b_1 \left[\prod_{i=1}^{d} \frac{(n-i+2)}{(n-1)^d} - b_1 \right]$$

obtained from the general moment formula of section 2.1, after some algebra (see also, Djauhari, 2005, 2008).

The corresponding empirical limits are given by

$$LCL = |\bar{S}|/b_3 \left(b_1 - 3\sqrt{b_2}\right) \quad ; \quad UCL = |\bar{S}|/b_3 \left(b_1 + 3\sqrt{b_2}\right) \qquad \text{where}$$

$$b_3 = \frac{1}{[m(n-1)]^d} \prod_{i=1}^{d} [m(n-1) - i + 1]$$

and $\bar{S}$ is the matrix of average variances and covariances based on m calibration samples (phase I). These formulae will be applied in the two numerical examples presented at section 5.

(ii) **false alarm α risk:** In the case of $d = 2$, we have the exact distribution for $|S|$ in simple form (given at 2.1 *(ii)*), where $|\Sigma| = |\Sigma_0|$ under H_0: $\Sigma = \Sigma_0$.

The reference value for α is the usual 0.0027, which is pre-fixed. However, the actual α risk, is given by

$$\begin{aligned} \alpha\, risk &= \mathbb{P}(Reject\, H_0 \,|\, H_0\, is\, true) = 1 - \mathbb{P}(LCL \le |S| \le UCL \,|\, H_0\, is\, true) \\ &= 1 - \mathbb{P}\left(|\Sigma_0| \left(b_1 - 3\sqrt{b_2} \right) \le \frac{|\Sigma_0|}{4(n-1)^2} \left(\chi^2_{2n-4} \right)^2 \le |\Sigma_0| \left(b_1 + 3\sqrt{b_2} \right) \right) \\ &= 1 - \left[F_{\chi^2_{2n-4}} \left(2(n-1)\sqrt{b_1 + 3b_2^{1/2}} \right) - F_{\chi^2_{2n-4}} \left(2(n-1)\sqrt{b_1 - 3b_2^{1/2}} \right) \right] \end{aligned}$$

For $d > 2$, the α risk is obtained numerically, by simulation of $|S|$, as shown in section 4.

3 The New $|S|$ and $tr(V)$ Control Charts

3.1 The $|S|$ Control Limits

In order to better approximate the exact distribution of the sample $|S|$ statistic, we correct its non-normality (skewness and kurtosis) using the information from the 3rd and 4th order cumulants of $|S|$ (K_3 and K_4 from section 2.1 *(iv)*), through the Cornish-Fisher expansion formula (Cornish & Fisher, 1960; Lee & Lee, 1992; www.riskglossary.com/link/cornish_fisher). In this formula, the p-quantile of $|S|^* = \frac{|S|-\mu}{\sigma}$, denoted $q_{|S|^*}(p)$, is corrected, starting from the p-quantile of $Z \sim N(0,1)$, denoted $q_Z(p)$, as follows:

$$q_{|S|^*}(p) \approx q_Z(p) + K_3 \frac{q_Z^2(p) - 1}{6} + K_4 \frac{q_Z^3(p) - 3q_Z(p)}{24} - K_3^2 \frac{2q_Z^3(p) - 5q_Z(p)}{36}$$

Since $|S| = \mu + \sigma |S|^*$, then $q_{|S|}(p) = \mu + q_{|S|^*}(p)\, \sigma = b_1 |\Sigma| + q_{|S|^*}(p) \sqrt{b_2 |\Sigma|^2}$, and the CF quantile formula is: $q_{|S|}(p) = |\Sigma| \left[b_1 + q_{|S|^*}(p) \sqrt{b_2} \right]$, where $p = \frac{\alpha_0}{2} = 0.00135$ and $p = 1 - \frac{\alpha_0}{2} = 0.99865$ will give the two-sided control limits of the chart. Note that this new expression has the same structure as the normal control limits (see 2.2 *(i)*), but with $q_{|S|^*}$ substituted for the values 3 and -3. For the important case of one-sided upper control limit, $p = 1 - \alpha_0 = 0.9973$.

The Table 2 below gives the numerical values of these CF corrected quantiles of $|S|$ in standardized form, for dimension $d = 3$, considering only one correction term (skewness correction).

Table 2: **Quantiles of Standardized** $|S|^*$
$d = 3$, $\alpha_0 = 0.0020$ **and** 0.0027

n	$1-\alpha_0$		n	$1-\alpha_0$	
	0.9980	**0.9973**		**0.9980**	**0.9973**
15	5.43891	5.15184	23	4.78027	4.54234
16	5.31938	5.04123	24	4.72861	4.49454
17	5.21470	4.94435	25	4.68089	4.45037
18	5.12208	4.85864	26	4.63663	4.40941
19	5.03941	4.78214	27	4.59543	4.37129
20	4.96506	4.71334	28	4.55696	4.33570
21	4.89773	4.65104	29	4.52094	4.30236
22	4.83642	4.59430	30	4.48712	4.27106

3.2 The $|S|$ Chart Performance: False Alarm α Risk

For dimension $d = 2$, since $|S| \sim \frac{|\Sigma|}{4(n-1)^2}(\chi^2_{2n-4})^2$, we have (two sided case)

$$\alpha\, risk = \mathbb{P}(Reject\ H_0 \,|\, H_0\ is\ true) = 1 - \mathbb{P}(LCL \leq |S| \leq UCL \,|\, H_0\ is\ true)$$

$$= 1 - \mathbb{P}(\underbrace{\left[b_1 + q_{|S|^*}(\alpha_0/2)\sqrt{b_2}\right]}_{CF_1}|\Sigma_0| \leq \frac{|\Sigma_0|}{4(n-1)^2}\left(\chi^2_{2n-4}\right)^2 \leq \underbrace{\left[b_1 + q_{|S|^*}(1-\alpha_0/2)\sqrt{b_2}\right]}_{CF_2}|\Sigma_0|)$$

$$= 1 - \mathbb{P}\left(2(n-1)\sqrt{CF_1} \leq \chi^2_{2n-4} \leq 2(n-1)\sqrt{CF_2}\right)$$

$$\alpha\, risk = 1 - \left[F_{\chi^2_{2n-4}}\left(2(n-1)\sqrt{CF_2}\right) - F_{\chi^2_{2n-4}}\left(2(n-1)\sqrt{CF_1}\right)\right]$$

where CF_1 is the lower CF quantile for $|S|$ and CF_2 is the upper CF quantile for $|S|$.

For the one-sided case, $\alpha\ risk = 1 - F_{\chi^2_{2n-4}}\left(2(n-1)\sqrt{CF_2}\right)$, where $\frac{\alpha_0}{2}$ is substituted by α_0 in the CF_2 expression.

For dimension greater than 2, the false alarm risk should be obtained numerically by simulation.

3.3 The $tr(V)$ Auxiliary Chart

Let´s consider a standardized form for the sample variance-covariance S matrix given by

$$V = N\Sigma_0^{-1/2} S \Sigma_0^{-1/2}, \qquad \text{where} \qquad \Sigma_0 = \bar{S} = \frac{1}{m}\sum_{i=1}^{m} S_i,$$

which is based on m calibration samples (with variance-covariance matrizes $S_i,\ i = 1, ..., m$) from the process under control ($\Sigma = \Sigma_0$), and $N = n - 1$. This covariance matrix standardization is very useful in statistics (see for instance Anderson, 1984; Korin, 1968) and can be easily implemented through the Singular Value Decomposition (which can be obtained in the

R software or Matlab by the function "eigen").

As a consequence, since S follows a Wishart distribution, then $V \sim Wishart(N, I)$ with identity shape matrix. This makes posible the simulation of trace(V) in order to obtain its quantiles (control limits for the tr(V) chart). Using the Wishart-variate generator of Matlab (Smith and Hocking, 1972), it was simulated 10 runs of 2 million samples for each N (N from 3 to 30 and $\alpha = 0.0020$ and $\alpha = 0.0027$), in order to obtain the table of upper quantiles (average of runs) of tr(V), which is given below (Table 3). The quantile variation among runs if sufficiently small (standard deviation $<< 0.1$), which guarantees a two or three digits precision.

Table 3: **Upper Quantiles of tr(V)**
$d = 3$, $\alpha_0 = 0.0020$ **and** 0.0027

N	$1-\alpha_0$		N	$1-\alpha_0$	
	0.9980	**0.9973**		**0.9980**	**0.9973**
3	20.07	20.79	17	79.77	81.09
4	25.27	26.05	18	83.61	84.96
5	30.11	30.96	19	87.39	88.77
6	34.71	35.61	20	91.22	92.60
7	39.17	40.14	21	94.97	96.40
8	43.53	44.51	22	98.72	100.22
9	47.74	48.78	23	102.44	103.95
10	51.93	53.02	24	106.15	107.66
11	56.04	57.18	25	109.90	111.39
12	60.10	61.30	26	113.60	115.16
13	64.11	65.30	27	117.25	118.79
14	68.05	69.31	28	120.86	122.53
15	71.97	73.27	29	124.57	126.23
16	75.88	77.17	30	128.18	129.83

4 False Alarm Comparative Study

4.1 The case of dimension $d = 2$

From previous sections (2.2 and 3.2), we have obtained the expressions for the exact false alarm risk for the traditional normal-based $|S|$ chart and the Cornish-Fisher corrected $|S|$ chart, which are (two-sided case)

$$\alpha\, risk\,(normal) = 1 - \left[F_{\chi^2_{2n-4}}\left(2(n-1)\sqrt{b_1 + 3b_2^{1/2}}\right) - F_{\chi^2_{2n-4}}\left(2(n-1)\sqrt{b_1 - 3b_2^{1/2}}\right)\right]$$

$$\alpha\, risk\,(CF\ corrected) = 1 - \left[F_{\chi^2_{2n-4}}\left(2(n-1)\sqrt{CF_2}\right) - F_{\chi^2_{2n-4}}\left(2(n-1)\sqrt{CF_1}\right)\right]$$

The ideal exact-distributed $|S|$ chart, taken as a reference, has obviously $\alpha\, risk = \alpha_0$, the pre-fixed risk of type-I (reject H_0 when H_0 is true), which is considered as the usual value 0.0027 . The comparison results, are presented in form of table and graphics as well, as a function of the sample size n, for two-sided and one-sided charts.

The table below (Table 4) shows the false alarm risks for two-sided charts for n from 3 to 60, and after that, the same results are presented graphically (Fig. 1).

Table 4: α **risk (two-sided)**

n	$Normal\ Approx.$	$Cornish-Fisher$	n	$Normal.Approx.$	$Cornish-Fisher$
3	0.01971	0.00061	9	0.01737	0.00225
4	0.02081	0.00096	10	0.01670	0.00392
5	0.02042	0.00117	15	0.01409	0.00467
6	0.01968	0.00130	20	0.01234	0.00395
7	0.01888	0.00139	30	0.01014	0.00336
8	0.01810	0.00144	60	0.00719	0.00297
ref.	**0.00270**	**0.00270**	**ref.**	**0.00270**	**0.00270**

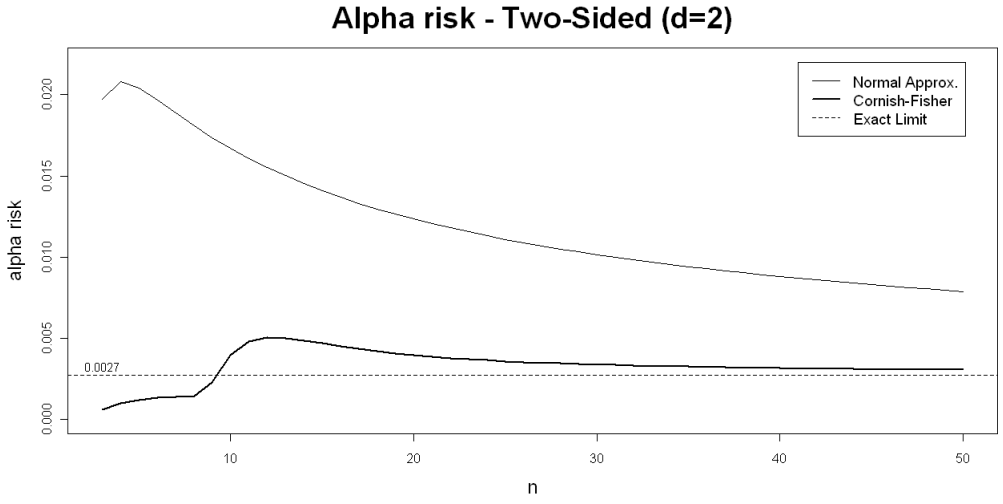

Figure 1: α risk of $|S|$ exact versus approximated normal versus Cornish-Fisher

From the table and figure above, it is clear that our corrected chart presents false alarm risks much closer to the reference risk ($\alpha_0 = 0.0027$) than the traditional normal-based chart.

If we consider only the upper risk (probability of crossing the upper limit when H_0 is true), since it is the more important risk, the comparative results are even stronger, in favor of the corrected chart, as shown in Figure 2 below.

And in this case, only one term of correction in the Cornish-Fisher formula is sufficient.

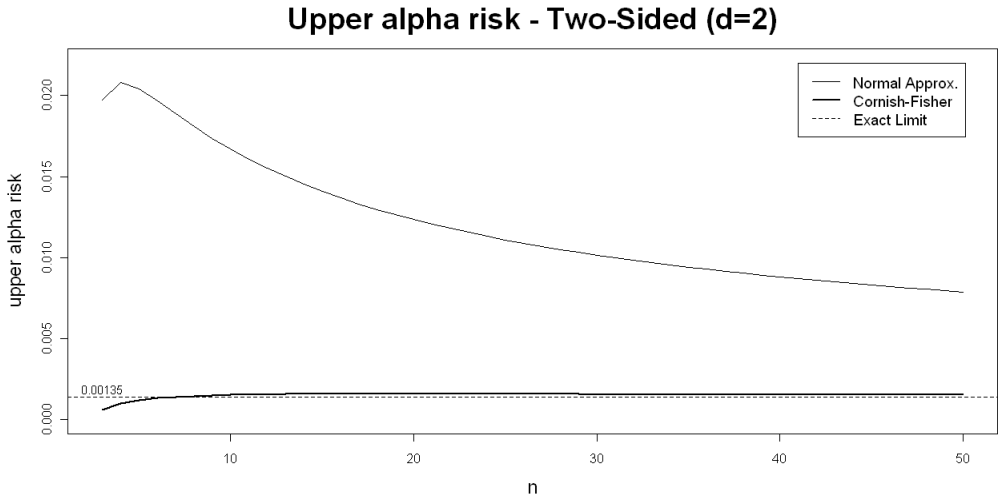

Figure 2: Upper α risk of $|S|$ exact versus approximated normal versus Cornish-Fisher

In this way, in the one-sided chart (only upper limit), we use only one correction term, and the results are presented below, at Table 5 and Figure 3.

Table 5: α **risk (one-sided)**

n	$Normal\ Approx.$	$Cornish-Fisher$	n	$Normal\ Approx.$	$Cornish-Fisher$
3	0.01971	0.00100	9	0.01737	0.00259
4	0.02081	0.00161	10	0.01670	0.00265
5	0.02042	0.00198	15	0.01409	0.00281
6	0.01968	0.00222	20	0.01234	0.00285
7	0.01888	0.00239	30	0.01014	0.00287
8	0.01810	0.00250	60	0.00719	0.00284
ref.	**0.00270**	**0.00270**	**ref.**	**0.00270**	**0.00270**

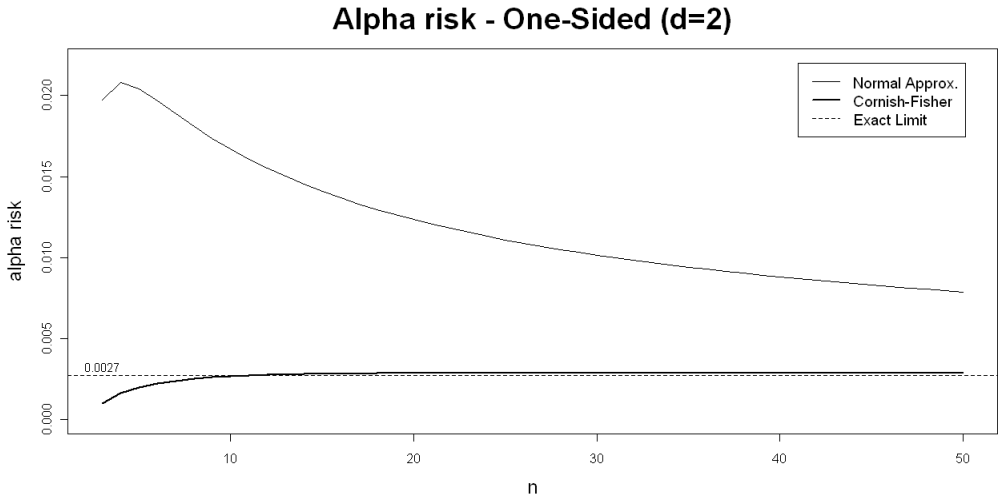

Figure 3: α risk (one-sided) of $|S|$ exact versus approximated normal versus Cornish-Fisher

From the table and figure above we can see that the correction (just one term) produce excellent results, where the excess of false alarm is substantially reduced, almost eliminated for $n \geq 8$ say.

4.2 The case of dimension $d = 3$

In this case, the α risks were obtained by simulation of the $|S|$ sample distribution, through a Wishart random generator (algorithm AS53, from Smith and Hocking, 1972) available in the Matlab software, considering around $N = 1$ million samples for each sample size n. Before the study with dimension 3, we have tested the simulator in the case of dimension 2, where we know the exact distribution. This distribution depends on the Σ parameter, and we have considered, without loss of generality, that $\Sigma = \begin{pmatrix} 1 & \rho \\ \rho & 1 \end{pmatrix}$, where the particular ρ value ($\rho = 0.5$ and 0.75 in the figures) does not have impact on the degree of approximation.

Just to illustrate the excellence of the method, with $n = 10$ and $N = 10^6$, we can not distinguish between the exact density of $|S|$ and the simulated one, as show at Figure 4 below.

Figure 4: **Density of $|S|$ exact versus simulated - $n = 10$, $N = 1$ million and $d = 2$**

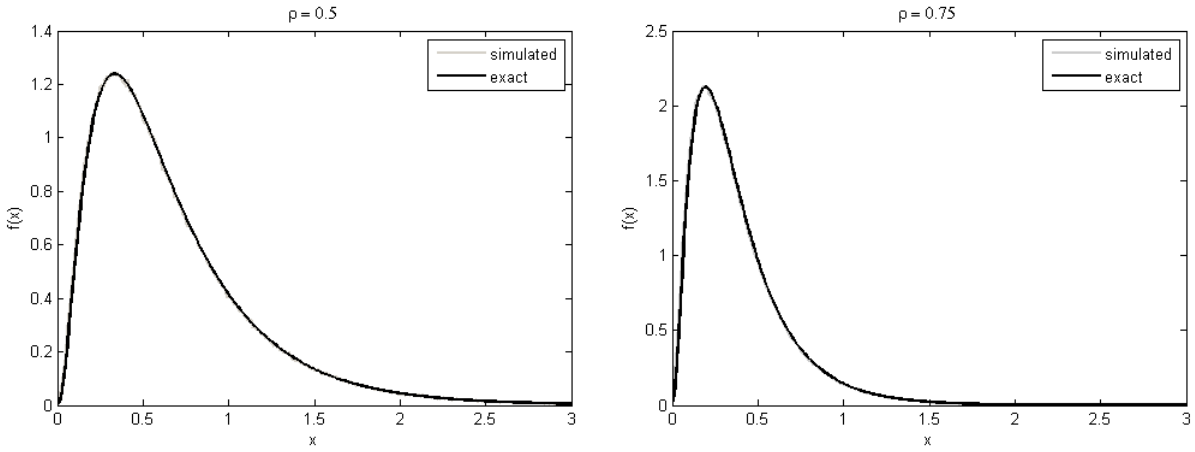

Based on this test, we have adopted the value $N = 10^6$. For dimension $d = 3$, we have considered just the one-sided (upper limit) chart, and CF correction with only one term. The results are shown bellow, at Table 6, where the quantiles from the 3 methods are presented, and at Figure 5 (for the false alarm risk).

Table 6: **Upper Quantiles (one-sided : $\alpha_0 = 0.0027$)**

n	$Exact(sim.)$	$Normal\ Approx.$	CF	n	$Exact(sim.)$	$NormalApprox.$	CF
4	2.68949	1.03849	5.50433	9	2.42403	1.30405	2.59090
5	2.89698	1.23081	4.23237	10	2.29517	1.29008	2.41570
6	2.82795	1.29575	3.54973	15	1.89068	1.21041	1.90241
7	2.68866	1.31462	3.11760	20	1.64740	1.14353	1.64311
8	2.53757	1.31384	2.81575	30	1.38473	1.04938	1.37043

From the table above, we can see that the Cornish-Fisher quantiles are closer to the exact quantiles than the normal ones; in particular, for $n = 15$ or more, the Cornish-Fisher approximation is very good.

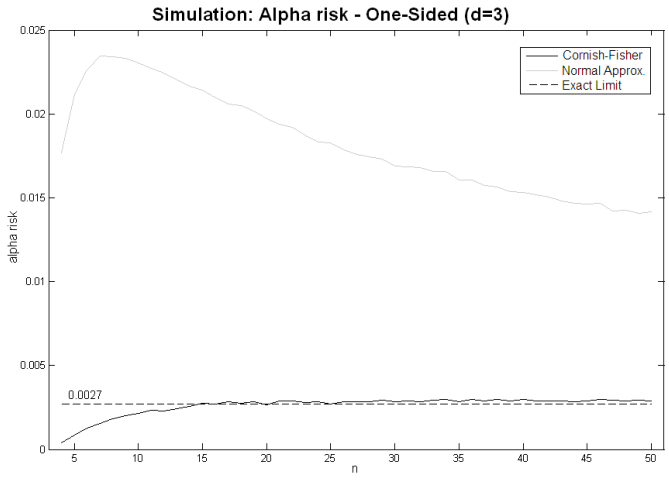

Figure 5: α risk (one-sided) of $|S|$ exact versus approximated normal versus Cornish-Fisher through simulations ($N = 1$ million samples for each sample size n)

From the figure above, we can see that this one term CF correction reduces almost all the excess of false alarm present in the normal-based chart.

5 Numerical Illustrations

5.1 An Example with $d = 2$

In order to illustrate the application of our corrected $|S|$ chart with real data, we consider an adaptation of the example 11.1 from Montgomery (2008). The tensile strength and diameter of a textile fiber are two important quality characteristics that are to be jointly controlled. The quality engineer has decided to use $n = 10$ fiber specimens in each sample. He has taken 20 preliminary samples whose variances, covariances and corresponding matrix determinants are shown in Table 7 below.

Table 7: **Variability data for the textile fiber example - d=2**

k	S^2_{1k}	S^2_{2k}	S_{12k}	$\lvert S_k\rvert$	k	S^2_{1k}	S^2_{2k}	S_{12k}	$\lvert S_k\rvert$
1	1.25	0.87	0.80	0.4475	11	1.45	0.79	0.78	0.5371
2	1.26	0.85	0.81	0.4149	12	1.24	0.82	0.81	0.3607
3	1.30	0.90	0.82	0.4976	13	1.26	0.55	0.72	0.1746
4	1.02	0.85	0.81	0.2109	14	1.17	0.76	0.75	0.3267
5	1.16	0.73	0.80	0.2068	15	1.48	1.07	0.82	0.9112
6	1.01	0.80	0.76	0.2304	16	1.74	1.27	0.83	1.5209
7	1.25	0.78	0.75	0.4125	17	1.80	1.42	0.70	2.0660
8	1.40	0.83	0.80	0.5220	18	1.42	1.00	0.79	0.7959
9	1.19	0.87	0.83	0.3464	19	1.31	0.89	0.76	0.5883
10	1.17	0.86	0.95	0.1037	20	1.29	0.85	0.68	0.6341

Based on the table above (preliminary samples), taking the average of the variances and covariances of all these samples, we obtain an estimate of Σ, given by

$$\bar{S} = \begin{pmatrix} \bar{S}_1^2 & \bar{S}_{12} \\ & \bar{S}_2^2 \end{pmatrix} = \begin{pmatrix} 1.3025 & 0.7885 \\ & 0.8835 \end{pmatrix}$$

which results in $|\bar{S}| = 0.5290$. The constants b_1, b_2 and b_3 are given by

$$b_1 = \frac{(n-2)}{(n-1)} = 0.8889 \quad ; \quad b_2 = \frac{(n-2)(4n-2)}{(n-1)^3} = 0.4170 \quad \text{and} \quad b_3 = \frac{m(n-1)-1}{m(n-1)} = 0.9944$$

since $n = 10$. As $|\bar{S}|$ is a biased estimator of $|\Sigma|$ we consider its bias-corrected version (see Djauhari, 2008), given by $\widehat{|\Sigma|} = |\bar{S}|/b_3 = 0.5290/0.9944 = 0.5320$, as the corresponding numerical value for $|\Sigma|$ in the control limits expression.

Let's consider the one-sided case, where the upper limits for the 3 charts (normal-based, CF corrected and exact limits), are given by:
(i) normal-based: $UCL = \widehat{|\Sigma|}\left(b_1 + q_Z(0.9973)\sqrt{b_2}\right) = 1.4286$
(ii) CF corrected: $UCL = q_{|S|}(0.9973) = \widehat{|\Sigma|}\left[b_1 + q_{|S|^*}(0.9973)\sqrt{b_2}\right] = 2.1602$
(iii) exact limit: $UCL = \widehat{|\Sigma|}(q_{\chi^2_{2n-4}(0.9973)})^2/4(n-1)^2 = 2.1536$

The figure 6b below illustrate this situation, where the CF corrected chart practically coincide with the exact limit chart, avoiding the false alarm drawback that happens with the traditional normal-approximated $|S|$ control chart. In this case, the figure shows that there is no sign of problems with the process variability (see also figure 6d) nor with the process level (figure 6a) expressed through the Hotelling statistic. Also, the auxiliary $tr(V)$ chart confirms the stability of the Σ matrix suggested by the $|S|$ chart.

Figure 6a: **Hotelling T^2 Control Chart - One-Sided,** $d = 2$

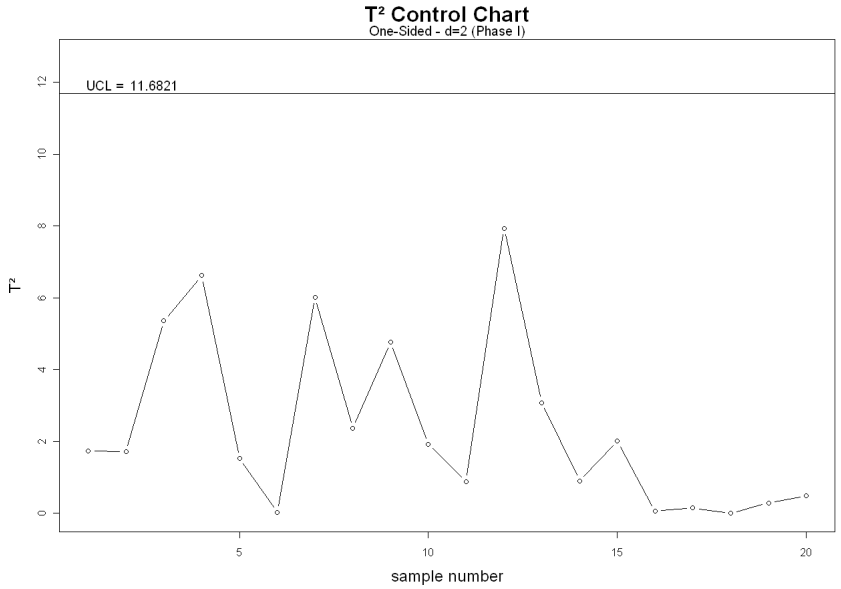

Figure 6b: $|S|$ **Control Chart - One-sided,** $d = 2$

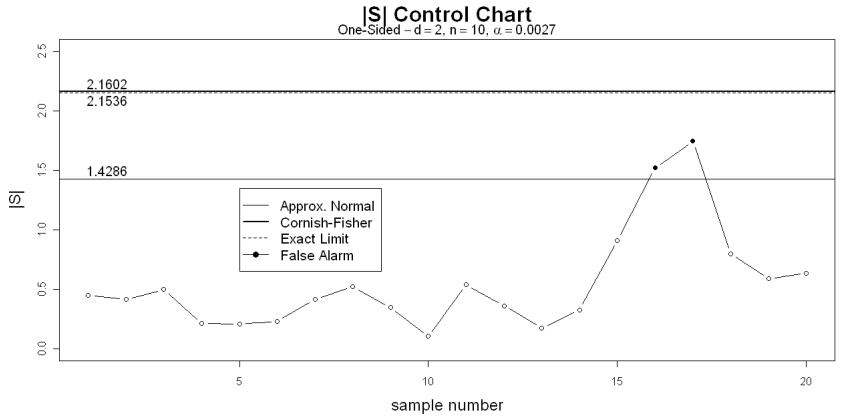

5.2 An Example with $d = 3$

In order to illustrate the application of the proposed $|S|$ corrected chart when $d = 3$, we consider one adaptation of case 1 of Fuchs and Kenett (1998) where some simulations were made from the original multivariate data in order to get samples of size $n = 15$.

These original data are from a capability study of a process to produce aluminium bolts, which were used as base to generate 70 simulated samples of dimension $d = 3$. A sketch of these aluminium bolts and the variables measured (X_1, X_2, X_3) is presented in the picture below.

The first 30 samples (from the total of 70) were generated by simulation from the first 5 original samples, in order to be used as calibration samples for the phase I (control

Figure 6c: $tr(V)$ **Control Chart - One-sided,** $d = 2$

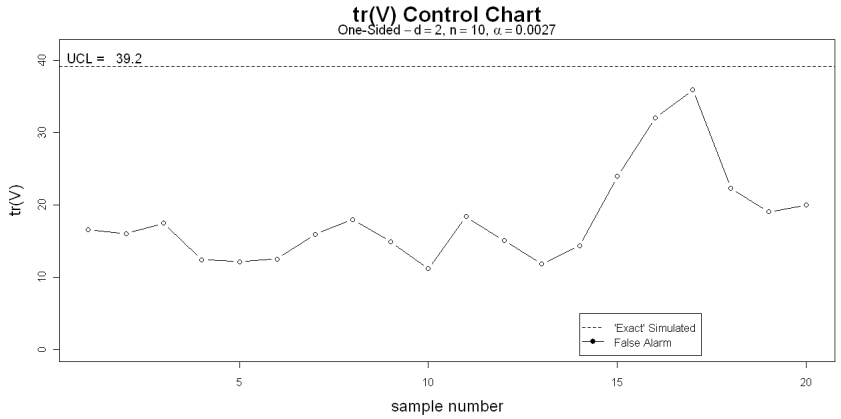

Figure 6d: S_1^2 **and** S_2^2 **Control Chart - One-Sided**

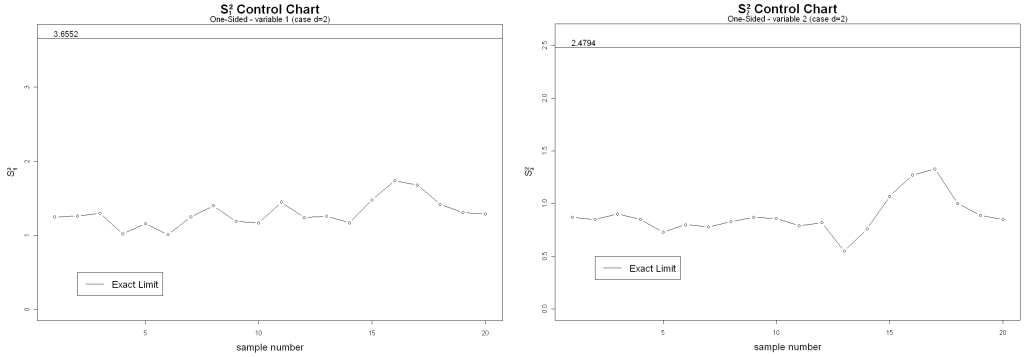

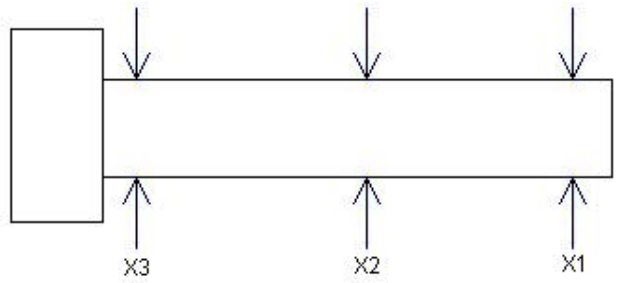

Figure 7: Aluminium bolt sketch and the measured variables

chart implementation). From these original samples, the parameters (means, variances and covariances) used in the simulation were obtained as shown at table 8 below.

The multivariate normal samples simulated based on the parameters above (table 8) were multiplied by 100, and then computed the $|S|$ statistic for each sample; as shown at table 9 below (Case A). Table 10 (Case B) was generated in the same basic way that table 9, but at phase II the variance-covariance parameters (from table 8) in the last line were increased by 20% in order to design an out of control case.

Table 8: **Parameters used in the simulation -** $d = 3$

k	μ_{1k}	μ_{2k}	μ_{3k}	$S^2_{1k}\,(10^{-4})$	$S^2_{2k}\,(10^{-4})$	$S^2_{3k}\,(10^{-4})$	$S_{12k}\,(10^{-4})$	$S_{13k}\,(10^{-4})$	$S_{23k}\,(10^{-4})$
1	9.997	9.986	9.989	3.81	6.54	4.21	2.78	1.55	2.26
2	9.997	9.993	9.989	3.64	8.35	4.27	1.86	0.46	1.39
3	10.001	9.991	9.985	4.12	5.69	4.41	1.12	1.57	1.49
4	9.998	9.988	9.992	4.03	3.74	3.46	1.46	1.83	2.76
5	10.003	9.990	9.989	3.67	6.57	4.49	1.50	1.02	2.50

Table 9: **(Case A) Generated values of the sample** $|S|$ **statistic -** $d = 3$

Sample k	S^2_{1k}	S^2_{2k}	S^2_{3k}	S_{12k}	S_{13k}	S_{23k}	$\lvert S_k\rvert$
1	3.1162	6.5834	6.1119	3.5096	1.6776	4.3880	23.2470
2	2.9931	3.2691	2.4252	1.7599	0.8574	1.0699	13.6185
3	4.2850	7.7592	3.0955	2.7945	1.5054	2.4075	56.5838
⋮	⋮	⋮	⋮	⋮	⋮	⋮	⋮
30	6.3306	8.6488	3.6088	2.4109	1.1236	4.1597	78.6949
Sum	127.0971	183.7933	118.0057	44.3205	35.7878	70.1959	
Mean	4.2366	6.1264	3.9335	1.4773	1.1929	2.3399	**69.8438**

From the table margins (mean values), the average generalized variance matrix $\bar{S}$ is given by

$$\bar{S} = \begin{pmatrix} \bar{S}_1^2 & \bar{S}_{12} & \bar{S}_{13} \\ & \bar{S}_2^2 & \bar{S}_{23} \\ & & \bar{S}_3^2 \end{pmatrix} = \begin{pmatrix} 4.2366 & 1.4773 & 1.1929 \\ & 6.1264 & 2.3399 \\ & & 3.9335 \end{pmatrix}$$

resulting in $|\bar{S}| = 69.8438$. Since $|\bar{S}|$ is a biased estimator of $|\Sigma|$, the control limits are corrected by the constants (section 2.2),

$$b_1 = \frac{(n-2)(n-3)}{(n-1)^2} = 0.7959 \quad ; \quad b_2 = \frac{(n-2)(n-3)6}{(n-1)^3} = 0.3411$$

$$\text{and} \qquad b_3 = \frac{[m(n-1)-1][m(n-1)-2]}{[m(n-1)]^2} = 0.9929$$

Then, the control limits (normal, CF corrected and exact), considering $\widehat{|\Sigma|} = |\bar{S}|/b_3$, are given by

(i) normal-approximated: $UCL = \widehat{|\Sigma|}\left(b_1 + q_Z(0.9973)\sqrt{b_2}\right) = 170.294$

(ii) Cornish-Fisher corrected: $UCL = \widehat{|\Sigma|}\left[b_1 + q_{|S|^*}(0.9973)\sqrt{b_2}\right] = 267.652$

where $q_{|S|^*}(0.9973)$ was obtained from table 2 (section 3.1).

(iii) exact limit: $UCL = \widehat{|\Sigma|}\, x_0 = 265.462$

where $x_0 = 3.772$ was obtained integrating numerically the $h(y)$ density (table 1 at section 2.1 *(ii)*) using the *"meijerG"* function from the Matlab Symbolic Math Toolbox version 5.

From figure 8b below it is clear that the alarm from the normal chart should be considered a false alarm at the established α risk of 0.0027, since the exact limit is not reached by

any point. The CF corrected chart does not present this drawback since its UCL practically coincides with the exact limit.

Therefore, the figure shows that there is no evidence of process change in variability (see also Figures 8d for the univariate charts) as well as no change in the process level (Figure 8a) as expressed by the Hotelling statistic. Notice that one univariate chart can overcome slightly the limits without suggesting out of control, since a global α risk of 0.0027 would imply in individual control limits a bit larger. Also, the auxiliary $tr(V)$ chart at Figure 8c confirms the process dispersion stability suggested by the $|S|$ control chart.

Figure 8a: **Hotelling T^2 Control Chart - One-Sided, $d = 3$ (Case A)**

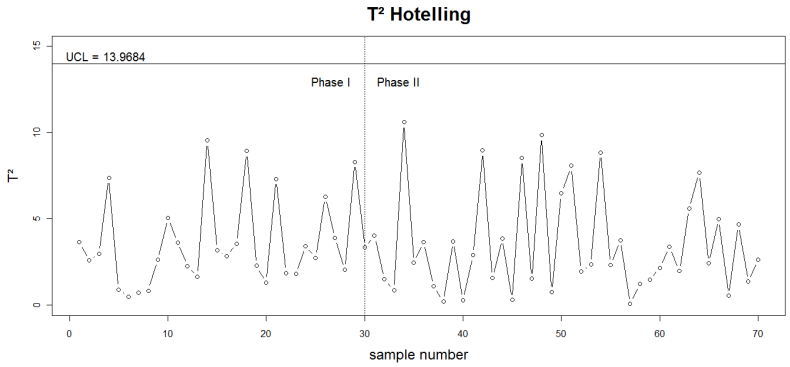

Figure 8b: **$|S|$ Control Chart - One-Sided, $d = 3$ (Case A)**

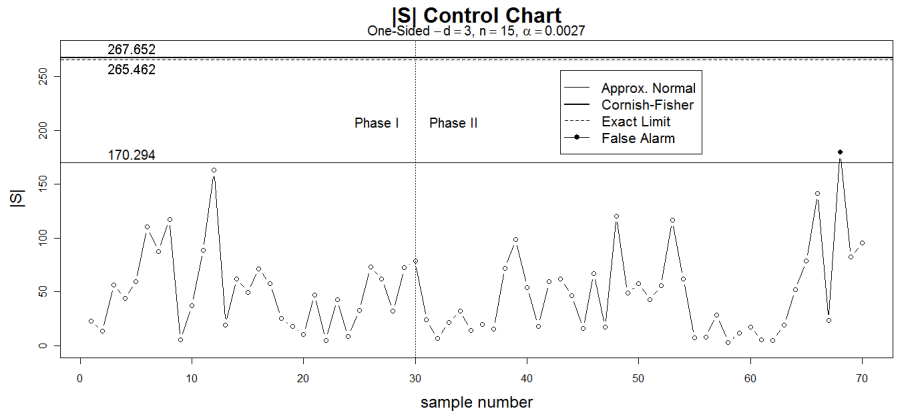

Figure 8c: $tr(V)$ **Control Chart - One-Sided,** $d = 3$ **(Case A)**

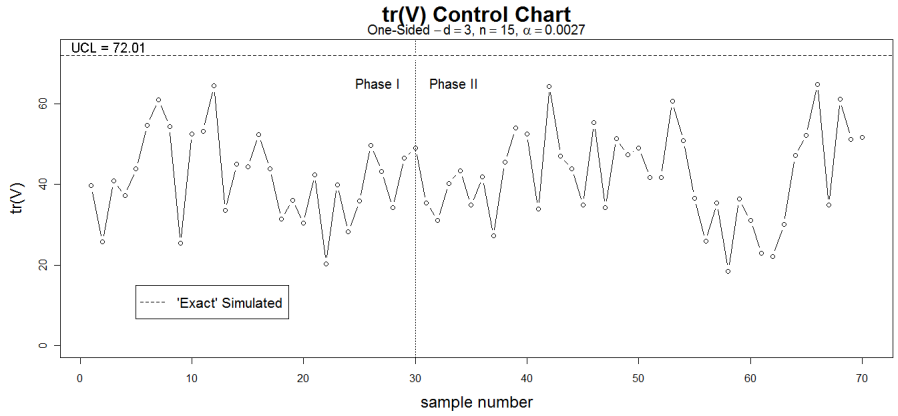

Figure 8d: **Univariate Variance** S^2 **Control Chart (Case A)**

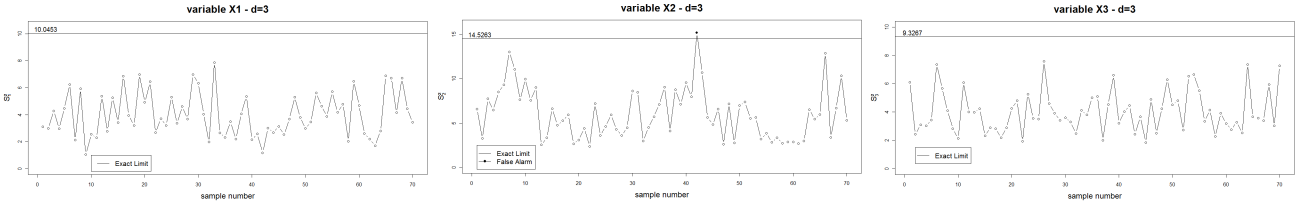

Table 10: **(Case B) Generated values of the sample** $|S|$ **statistic -** $d = 3$

Sample k	S^2_{1k}	S^2_{2k}	S^2_{3k}	S_{12k}	S_{13k}	S_{23k}	$\lvert S_k \rvert$
1	6.5655	8.3268	5.3509	4.5012	2.5334	2.2412	148.8112
2	2.7291	4.8125	3.4506	1.4738	0.0086	-0.9894	35.1273
3	3.4472	7.3501	4.2876	3.7593	0.5867	2.8692	29.7893
⋮	⋮	⋮	⋮	⋮	⋮	⋮	⋮
30	3.3491	8.7815	3.9405	3.7142	1.9587	2.2112	43.6371
Sum	120.3349	176.7983	116.7258	53.5943	37.4534	51.5648	
Mean	4.0112	5.8933	3.8909	1.7865	1.2484	1.7188	**66.1893**

From Table 10 B (mean values), the average generalized variance matrix $\bar{S}$ is given by

$$\bar{S} = \begin{pmatrix} \bar{S}_1^2 & \bar{S}_{12} & \bar{S}_{13} \\ & \bar{S}_2^2 & \bar{S}_{23} \\ & & \bar{S}_3^2 \end{pmatrix} = \begin{pmatrix} 4.0112 & 1.7865 & 1.2484 \\ & 5.8933 & 1.7188 \\ & & 3.8909 \end{pmatrix}$$

resulting in $|\bar{S}| = 66.1893$. Since $|\bar{S}|$ is a biased estimator of $|\Sigma|$, the control limits are corrected by the constants b_1, b_2 and b_3 previously presented (the same numerical values).

Then, the control limits (normal, CF corrected and exact), considering $\widehat{|\Sigma|} = |\bar{S}|/b_3$, are given by

(i) normal-approximated: $UCL = \widehat{|\Sigma|}\left(b_1 + q_Z(0.9973)\sqrt{b_2}\right) = 161.383$

(ii) Cornish-Fisher corrected: $UCL = \widehat{|\Sigma|}\left[b_1 + q_{|S|^*}(0.9973)\sqrt{b_2}\right] = 253.647$
where $q_{|S|^*}(0.9973)$ was obtained from table 2 (section 3.1).

(iii) exact limit: $UCL = \widehat{|\Sigma|}\, x_0 = 251.572$

where $x_0 = 3.772$ was obtained integrating numerically the $h(y)$ density (table 1 at section 2.1 *(ii)*) using the *"meijerG"* function from the Matlab Symbolic Math Toolbox version 5.

From figure 9b below it is clear that the $|S|$ chart was not able to detect the state of "out of control" given by the increase in the variance-covariance parameters used in the data simulation. However, the $tr(V)$ auxiliary chart (figure 9c) was able to detect this structural change in the process dispersion, helping the $|S|$ chart in his job. Also, the increase in process variability can be confirmed from the univariate charts (figures 9d), since one of then has shown an expressive signal of out of control; on the other hand, the Hotelling chart (figure 9a) shows the stability of process mean.

Figure 9a: **Hotelling T^2 Control Chart - One-Sided, $d = 3$ (Case B)**

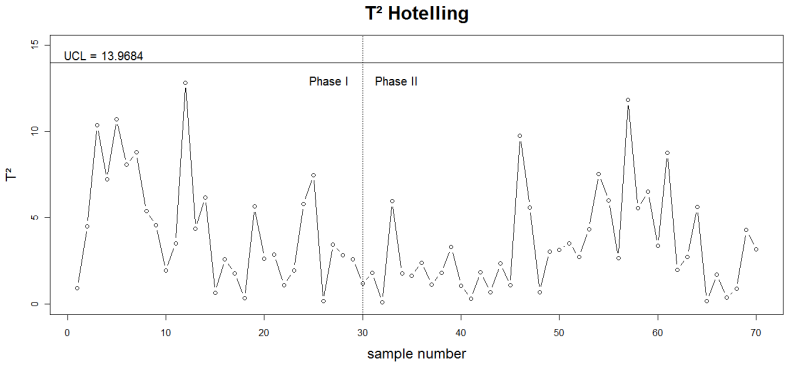

Figure 9b: $|S|$ **Control Chart - One-Sided, $d = 3$ (Case B)**

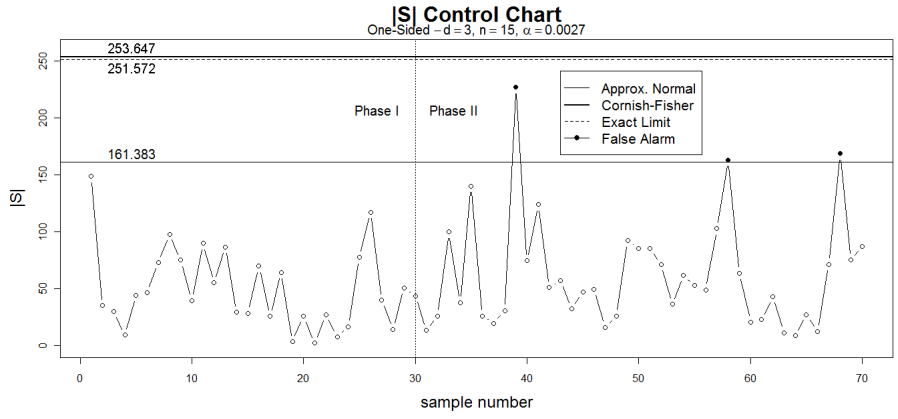

Figure 9c: $tr(V)$ **Control Chart - One-Sided,** $d = 3$ **(Case B)**

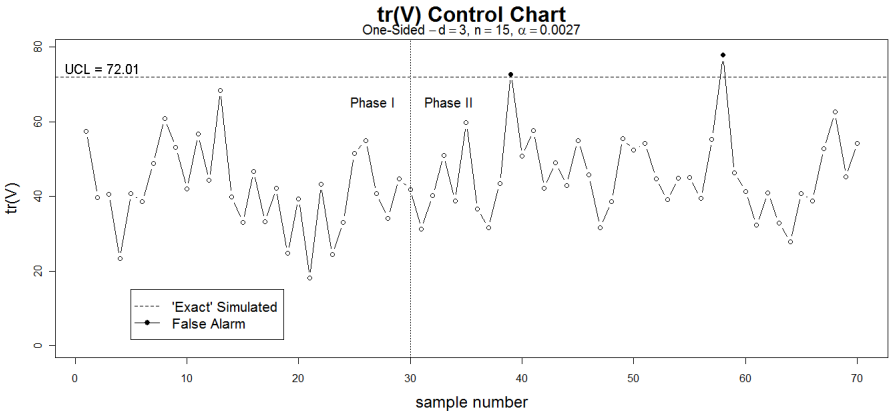

Figure 9d: **Univariate Variance** S^2 **Control Chart (Case B)**

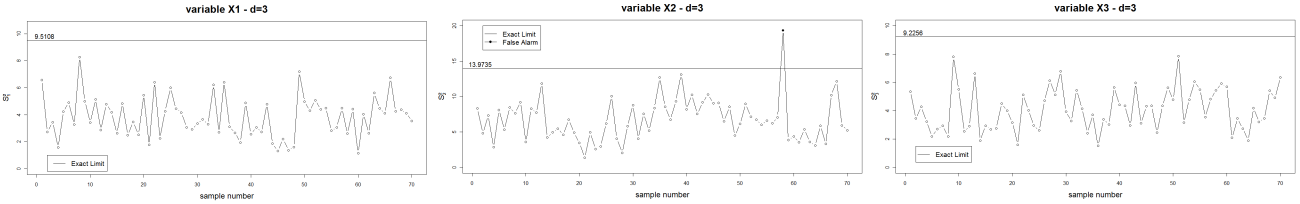

6 Final Comments and Conclusions

This paper has presented a simple correction in the traditional normal based $|S|$ control chart for multivariate process dispersion monitoring based on the Cornish-Fisher expansion formula. For the very important case of a one-sided chart with dimension $d = 3$, the correction is based on only one term involving the 3^{rd} order moment or cumulant, with a very simple implementation. Also, the basic limitation of the $|S|$ statistic (not detecting certain changes in the Σ matrix) is now alleviated with the introduction of an auxiliary $\text{tr}(V)$ chart, where V is the sample standardized variance-covariance S matrix.

At the same time, the gain in terms of practically eliminating the excess of false alarm of the traditional $|S|$ chart is enormous. With this new chart we can now control the false alarm risk at the pre-fixed level, avoiding the serious consequences of a non-controlled increase of this risk. For small or moderate sample sizes the correction works very well, and for very small samples, the quantiles of the exact $|S|$ distribution based on the Meijer G function (shown at Table 1) can be used.

7 Further Research

Although, for economy of space, we have presented only two numerical applications of the proposed methods with real data (with dimensions $d = 2$ and $d = 3$), the new methods

are valid and applicable to higher dimensions and we are presently extending the aluminium bolts example to the case of dimension $d = 4$.

Also, we are considering to extend the applicability of the methods proposed here in two directions. First, creating more facilities to the use of the Meijer G function (implementing it in the R software) in order to be able to deal with the case of extremely small n sample sizes. Second, to deal with the case of $d > n$.

8 Acknowledgements

The authors are grateful to the Universidade Estadual de Campinas (UNICAMP) and the Brazilian agency CNPq for a grant to the third author.

9 References

- Alt, F.A. (1984). "Multivariate Quality Control". In S. Kotz; N.L. Johnson, C.R. Reid, eds. *The Encyclopedia of Statistical Sciences*: pp. 110–122, Wiley, NY.
- Alwan, L. and Roberts, H.V. (1995). "The Problem of Misplaced Control Limits". *Applied Statistics*, 44, pp. 269–278.
- Anderson, T.W. (1958, 1984, 2003). *An Introduction to Multivariate Statistical Analysis.* Wiley.
- Aparisi, F.; Jabaloyes, J. and Carrión, A. (1999). "Statistical Properties of the $|S|$ Multivariate Control Chart." *Communications in Statistics - Theory and Methods*, 28 (11): pp. 2671–2686.
- Bateman, H. and Erdéryi, A. (1953) *Higher Trascendental Functions*, Vol 1 (PDF). New York: Mc Graw-Hill.
- Cavalcanti, A.B. and Cordeiro, G.M. (2006). An Improved u-Chart for Attributes. *Braz. J. of Prob. and Statist.* Vol 20, pp. 133-140.
- Chan, L. K. and Cui, H. J. (2003). "Skewness Correction X-bar and R charts for Skewed Distributions". *Naval Research Logistics*, 50 (6), pp. 555–573.
- Cornish, E.A. and Fisher, R.A. (1960). "The Percentage Points of Distributions Having Known Cumulants". *Technometrics*, 2: pp. 209–225.
- Djauhari, M.A. (2005). "Improved Monitoring of Multivariate Process Variability". *Journal of Quality Technology*, 37 (1): pp. 32–39.

- Djauhari, M. A.; Mashury, M. and Herwindiati, D. E. (2008). "Multivariate Process Variability Monitoring". *Communications in Statistics - Theory and Methods*, Vol. 37 (11), pp. 1742–1754.
- Dogu, E. and Kocakoç, I. D. (2011). "Estimation of Change Point in Generalized Variance Control Chart", *Communications in Statistics: Simulation and Computation*, 40: pp. 345–363.
- Fuchs, C. and Kenett, R. (1998). *Multivariate Quality Control*, Marcel Dekker.
- Fujikoshi, Y.; Ulyanov, V. and Shimizu, R. (2010). *Multivariate Statistics*, Wiley.
- Hotelling, H. (1931). "The Generalization of Student's Ratio". *Annals of Mathemathical Statistics*, vol. 2 (3): pp. 360–378.
- Hotelling, H. (1947). "Multivariate Quality Control". In: C. Eisenhart; M. Hastay, W.A. Wallis, eds. *Techniques of Statistical Analysis*. McGraw-Hill, NY, pp. 111–184.
- Joekes, S. and Barbosa, E. P. (2013). "An Improved Atribute Control Chart for Monitoring Non-Conforming Proportion in High Quality Processes". *Control Engineering Practice*, Vol 21 (4), pp. 407-412.
- Johnson, R.A. and Wichern, D.W. (2007). *Applied Multivariate Statistical Analysis*, 6^{th} ed., Pearson-Prentice Hall.
- Kabe, D.G. (1958) Some Applications of Meijer G-function to Distribution Problems in Statistics. *Biometrika*, Vol 45, No 3/4, pp. 578-580.
- Korin, B.P. (1968). "On the Distribution of a Statistic used for Testing a Covariance Matrix", *Biometrika*, Vol 55(1), pp. 171–178.
- Kruger, U. and Xie, L. (2012) *Statistical Monitoring of Complex Multivariate Processes*. Wiley.
- Lee, Y. and Lee, M.C. (1992). "On the Derivation and Computation of the Cornish-Fisher Expansion". *Australian Journal of Statistics*, 34 (3): pp. 443–450.
- Mason, R.L. and Young, J.C. (2001). *Multivariate Statistical Process Control with Industrial Applications*. Soc. for Industrial and Applied Mathematics.
- Mathai, A.M. (1972). "The Exact Non-Central Distribution of the Generalized Variance". *Annals of the Institute of Statical Mathematics*. 24: pp. 53–65.
- Matlab Matlab 2009. The MathWorks Inc, Symbolic Math Toolbox (version 5).

- Montgomery, D.C. (2012). *Introduction to Statistical Quality Control.* 7^{th} ed., Wiley.
- Pham-Gia, T. and Turkkan, N. (2010). "Exact Expression of the Density of the Sample Generalized Variance" *Statistical Papers*, 51 (4), pp. 931-945.
- R Development Core Team (2014). *R: A Language and Environment for Statistical Computing.* R Foundation for Statistical Computing, URL http://www.R-project.org
- Seber, G.A.F. (1984). *Multivariate Observations.* Wiley.
- Shewhart, W.A. (1926). "Quality Control Charts". *Bell System Tech. Journal* nº 5: pp. 593–603.
- Smith, W.B. and Hocking, R.R. (1972). "Algorithm AS53: Wishart Variate Generator". *JRSS, Series C (Applied Statistics)* vol 21, nº 3: pp. 341–345.
- Springer, M.D. (1979). *The Algebra of Random Variables*, Wiley, New York.
- Wilks, S.S. (1932). "Certain Generalizations in the Analysis of Variance". *Biometrika*, vol 24: pp. 471–494.
- Winterbottom, A. (1993). "Simple Adjustments to Improve Control Limits on Attribute Charts" *Quality and Reliability Engineering International*, 9(2), pp. 105-109.
- Woodall, W.H. (2000). "Controversies and Contradictions in Statistical Process Control", *Journal of Quality Technology*, Vol 32 (4), pp. 341-378.
- www.riskglossary.com/link/cornish_fisher.htm
- Yeh, A. B.; Lin, D. K. J. and McGrath, R. N. (2006). "Multivariate Control Charts for Monitoring Covariance Matrix: A Review". *Quality Technology and Qualitative Management*, 3, pp. 415-436.